

## Appendix B

### Appendix to Chapter 3: Impacts of the Graft Polymer Architecture on Physical Properties

1. Chang, A. B.;<sup>+</sup> Lin, T.-P.;<sup>+</sup> Thompson, N. B.; Luo, S.-X.; Liberman-Martin, A. L.; Chen, H.-Y.; Grubbs, R. H. Design, Synthesis, and Self-Assembly of Polymers with Tailored Graft Distributions. *J. Am. Chem. Soc.* **2017**, *139*, 17683–17693. (<sup>+</sup>*Equal contributions.*)
2. Lin, T.-P.;<sup>+</sup> Chang, A. B.;<sup>+</sup> Luo, S.-X.; Chen, H.-Y.; Lee, B.; Grubbs, R. H. Effects of Grafting Density on Block Polymer Self-Assembly: From Linear to Bottlebrush. *ACS Nano* **2017**, *11*, 11632–11641. (<sup>+</sup>*Equal contributions.*)
3. Haugan, I. N.; Maher, M. J.; Chang, A. B.; Lin, T.-P.; Grubbs, R. H.; Hillmyer, M. A.; Bates, F. S. Consequences of Grafting Density on the Linear Viscoelastic Behavior of Graft Polymers. *ACS Macro Lett.* **2018**, *7*, 525–530.

#### Table of Contents

<b>B-1</b> Characterization.....	203
<b>B-1.1</b> Instrumentation.....	204
<b>B-1.2</b> Determination of Grafting Density by <sup>1</sup> H NMR of Co-Monomer Mixtures	205
<b>B-1.3</b> Determination of $N_{bb}$ by SEC .....	207
<b>B-2</b> Supporting Data: Graft Distribution and Block Polymer Self-Assembly.....	208
<b>B-3</b> Supporting Data: Grafting Density and Block Polymer Self-Assembly .....	209
<b>B-4</b> Supporting Data: Grafting Density and Linear Rheology.....	219

#### **B-1 Characterization**

Many aspects of the characterization relevant to this chapter have been discussed in Appendix A, including <sup>1</sup>H NMR and SEC instrumentation (Appendix A-1) as well as standard procedures for determining copolymerization reactivity ratios (Appendix A-4). This section will first provide details for other measurements, including small-angle X-ray scattering and rheology, then describe how a combination of <sup>1</sup>H NMR and SEC can be used to determine the grafting density and total molecular weight.

### ***B-1.1 Instrumentation***

#### *Scanning Electron Microscopy*

Samples were prepared for SEM by fracturing films supported on glass to expose a cross-section, staining over ruthenium tetroxide vapors for 5 minutes, then coating with 5 nm Pd/Pt. SEM images were taken on a ZEISS 1550 VP Field Emission SEM.

#### *Small-Angle X-ray Scattering (SAXS)*

Sections 3-2 to 3-3: SAXS data were collected at Beamline 12-ID-B at Argonne National Laboratory's Advanced Photon Source. All polymers were thermally annealed at 140 °C for 24 hours under modest pressure and between Kapton films. The samples were studied using 12 keV (1.033 Å) X-rays, and the sample-to-detector distance was calibrated using a silver behenate standard. The beam was collimated using two sets of slits and a pinhole was used to remove parasitic scattering. The beamwidth was approximately 200–300 µm horizontally and 50 µm vertically.

Section 3-4: SAXS data were collected at Beamline 5-ID-D at Argonne National Laboratory's Advanced Photon Source. All polymers were dried under vacuum at elevated temperatures (> 100 °C) for several hours to remove any residual solvent, and bulk samples were mounted onto Kapton tape. The samples were studied using 0.729 Å X-rays, and the sample-to-detector distance was calibrated using a silver behenate standard.

#### *Differential Scanning Calorimetry (DSC): Section 3-4*

DSC data were collected by our collaborators at the University of Minnesota. Measurements were collected using TA Q1000 instrument equipped with a TA LNCS under dry N<sub>2</sub>. All polymers were dried under vacuum at elevated temperatures (> 100 °C) for several hours to remove any residual solvent prior to collecting data, then hermetically sealed at room temperature using Tzero pans. All samples were heated between 0 and 220 °C at a rate of 10 °C/min. The data reported was collected on the second heating cycle.

### *Linear Rheology: Section 3-4*

All rheology data were collected by our collaborators at the University of Minnesota using a Rheometric Scientific Ares 2 rheometer. The temperature was controlled by a forced convection oven. All samples were loaded onto 8 mm parallel plates and measured under dry nitrogen. Dynamic strain sweep analysis at 70 °C and 100 rad/s showed the linear viscoelastic regime persisted to 20% strain for all samples. (One exception: linear poly(DME) samples were measured at 100 °C.) Dynamic frequency sweep analysis was carried out from 70 to 200 °C (100–220 °C for linear DME samples) at a frequency range of 100–0.1 rad/s and a strain lower than the linear viscoelastic threshold. Master curves were prepared by shifting  $G^*$  along frequency axis to a reference of  $T_{\text{ref}} = T_g + 34$  °C, an arbitrary temperature to compare values of  $\eta_0$ .

### ***B-1.2 Determination of Grafting Density by $^1\text{H}$ NMR of Co-Monomer Mixtures***

For each sample, an aliquot of the macromonomer/diluent mixture was collected prior to initiating the polymerization. We note that in Sections 3-2 and 3-3, the samples are each block of the graft block polymer [*i.e.*, 3-3:  $(\text{PLA}^z\text{-}r\text{-DME}^{1-z})_n$ ,  $(\text{PLA}^z\text{-}r\text{-DBE}^{1-z})_n$ , or  $(\text{PS}^z\text{-}r\text{-DBE}^{1-z})_n$ ], whereas in Chapter 3-4, the samples are effectively graft homopolymers [*i.e.*,  $(\text{PLA}^z\text{-}r\text{-DME}^{1-z})_n$ ]. The following discussion will use  $(\text{PLA}^z\text{-}r\text{-DME}^{1-z})_n$  graft polymers as examples [ $M_n(\text{PLA}) = 3450$  g/mol].

The grafting density was determined from the relative  $^1\text{H}$  NMR integrations of the olefin resonances for the PLA macromonomer (6.30–6.25 ppm) and the discrete diluent (6.30–6.25, 6.10–6.05 ppm) in  $\text{CDCl}_3$ . Because the diluent resonances are centrosymmetric (*ddd*), the molar equivalents of the macromonomer and diluent are directly obtained by comparison. In turn, the grafting density is obtained from the mole fraction of the macromonomer. Representative spectra and calculations for the  $z = 0.15$  series are provided in Figure B.1 and Table B.1. For all samples, the calculated grafting densities were within 3% of the target values.

**Figure B.1:**  $^1\text{H}$  NMR spectra of the co-monomer mixtures for each  $(\text{PLA}^{0.15}\text{-}r\text{-DME}^{0.85})_n$  sample (Table 3.3) prior to initiation.

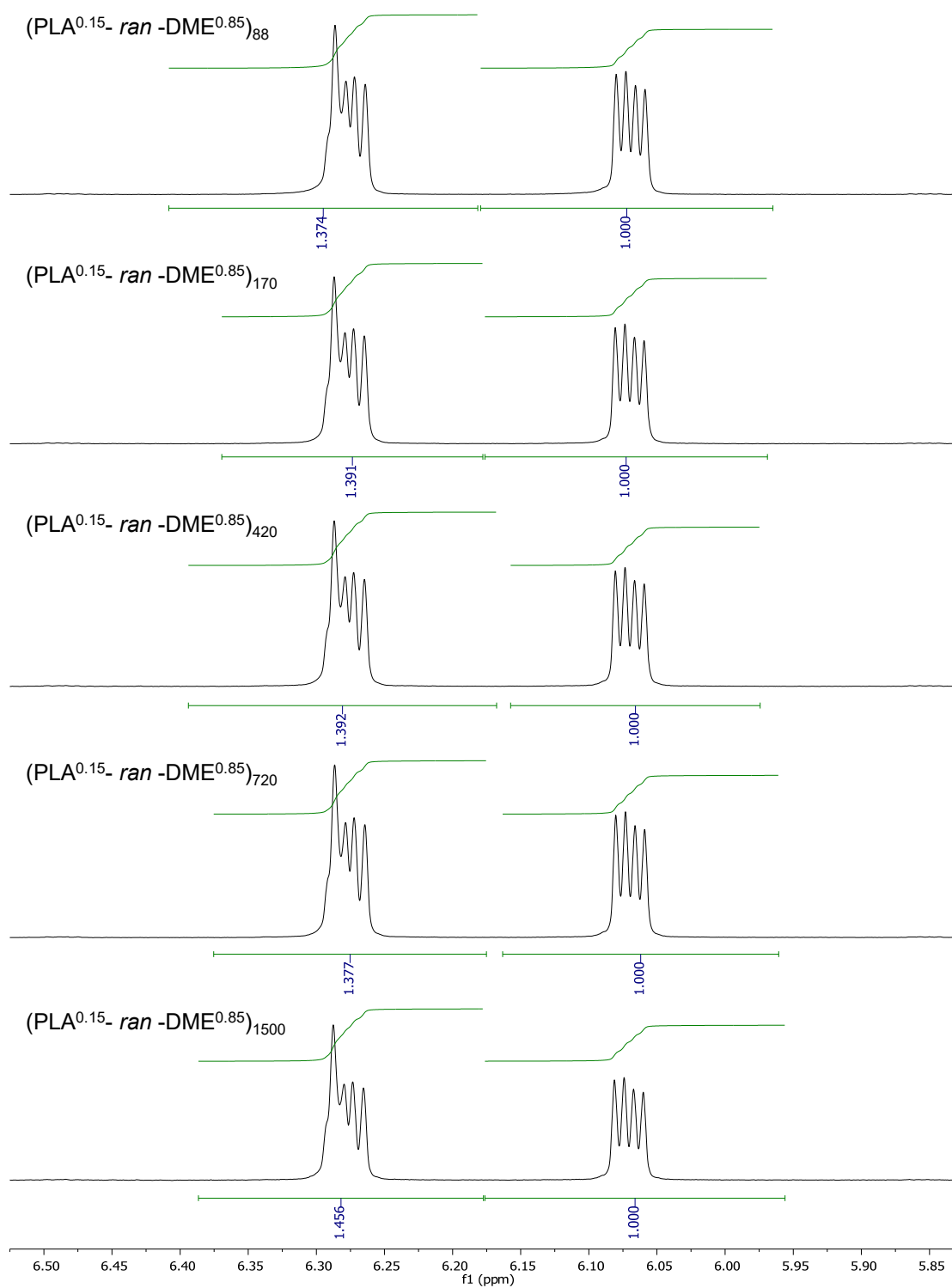




**Table B.1:** Representative calculations for the grafting density of each (PLA<sup>0.15</sup>-*r*-DME<sup>0.85</sup>)<sub>n</sub> sample (Table 3.3) from <sup>1</sup>H NMR analysis.

Sample ID	Integration (6.30–6.25 ppm)	Integration (6.10–6.05 ppm)	Equiv. MM	Equiv. DME	<i>z</i>
(PLA <sup>0.15</sup> - <i>ran</i> -DME <sup>0.85</sup> ) <sub>88</sub>	1.37	1.00	0.37	2.00	0.158
(PLA <sup>0.15</sup> - <i>ran</i> -DME <sup>0.85</sup> ) <sub>170</sub>	1.39	1.00	0.39	2.00	0.164
(PLA <sup>0.15</sup> - <i>ran</i> -DME <sup>0.85</sup> ) <sub>420</sub>	1.39	1.00	0.39	2.00	0.164
(PLA <sup>0.15</sup> - <i>ran</i> -DME <sup>0.85</sup> ) <sub>720</sub>	1.38	1.00	0.38	2.00	0.159
(PLA <sup>0.15</sup> - <i>ran</i> -DME <sup>0.85</sup> ) <sub>1500</sub>	1.45	1.00	0.45	2.00	0.185

### B-1.3 Determination of $N_{bb}$ by SEC

For each sample, a solution of known concentration (2 mg/mL) was prepared. The  $dn/dc$  values were determined by online measurements assuming 100% mass elution under the peak of interest. For all samples of the same grafting density, the  $dn/dc$  values were averaged and used to determine the weight-average total backbone degrees of polymerization,  $N_{bb}$ .

$N_{bb}$  is the sum of the weight-average backbone degrees of polymerization of the PLA macromonomer and DME diluent (*i.e.*,  $N_{bb} = N_{PLA} + N_{DME}$ ). The grafting density relates  $N_{PLA}$  and  $N_{DME}$ :

$$f = \frac{z}{1-z} = \frac{N_{PLA}}{N_{DME}} \quad \text{Eq. B-1}$$

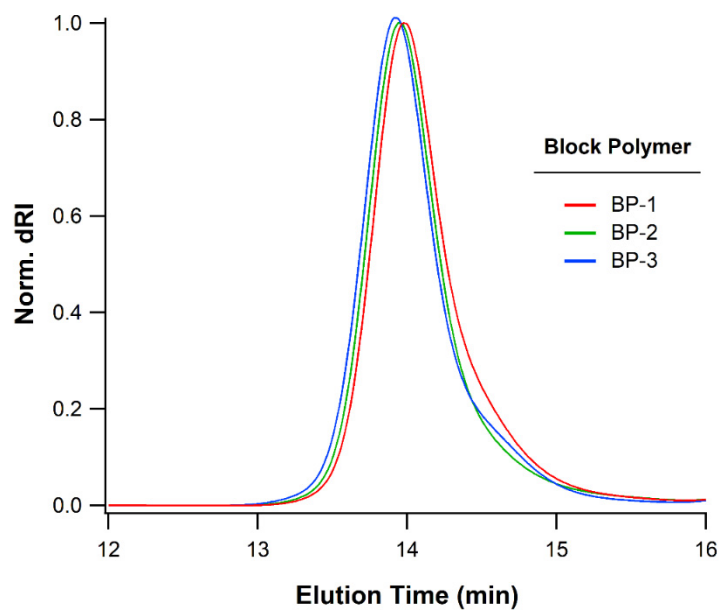
Eq. B-1 can be introduced into an expression for the weight-average total molar mass,  $M_w$ :

$$M_w = M_{PLA} n_{PLA} + M_{DME} n_{DME} = n_{DME} (M_{PLA} f + M_{DME}) \quad \text{Eq. B-2}$$

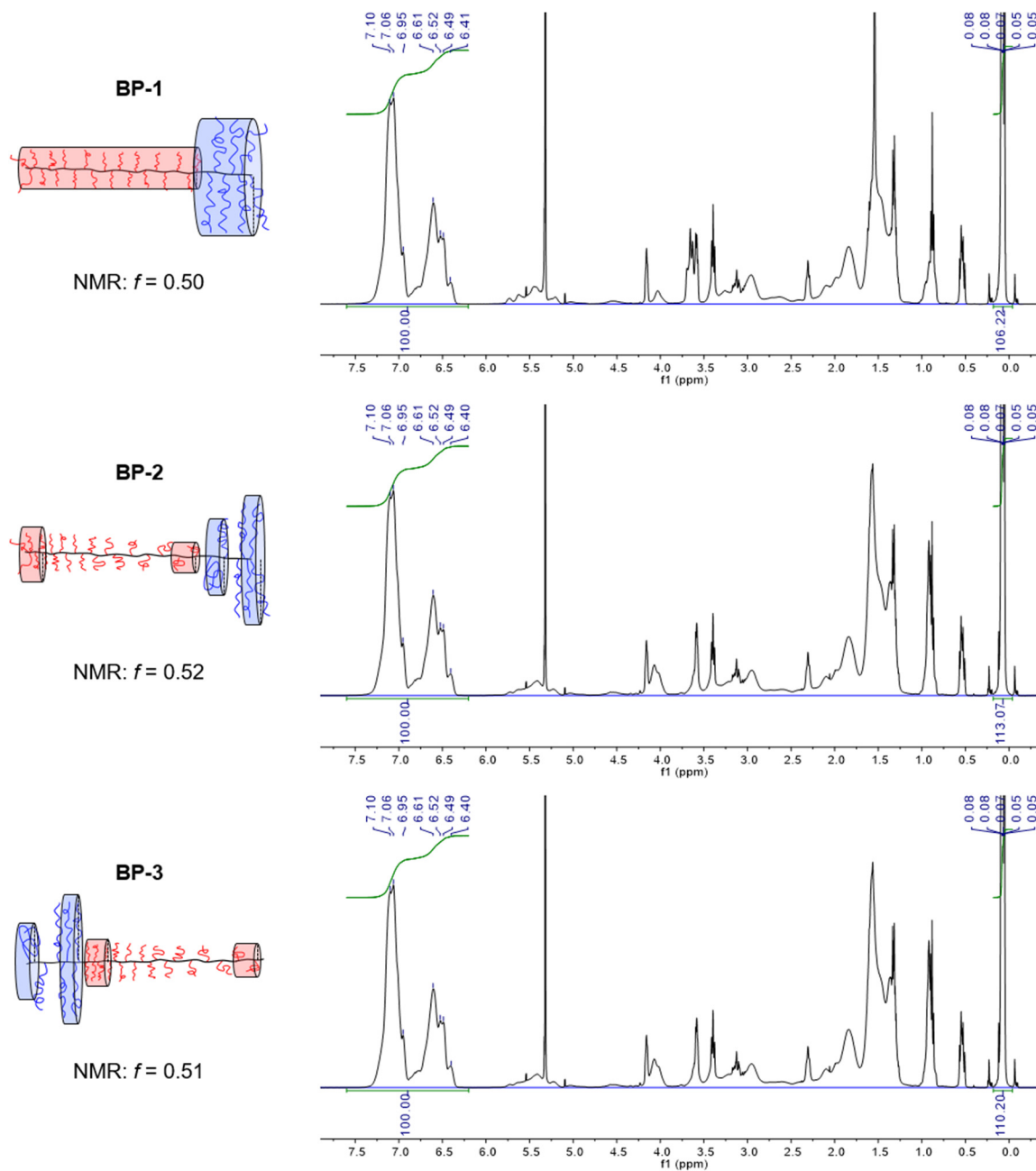
where  $M_{PLA}$  is the weight-average molar mass of the PLA macromonomer (3.45 kg/mol) and  $M_{DME}$  is the molar mass of the diluent (0.21 kg/mol).  $N_{DME}$  can be calculated using the  $M_w$  values determined by SEC:

$$n_{DME} = \frac{M_w \text{ (kDa)}}{3.45 f + 0.21} \quad \text{Eq. B-3}$$

From Eqs. B-1 and B-3,  $N_{PLA}$  and  $N_{bb}$  follow.

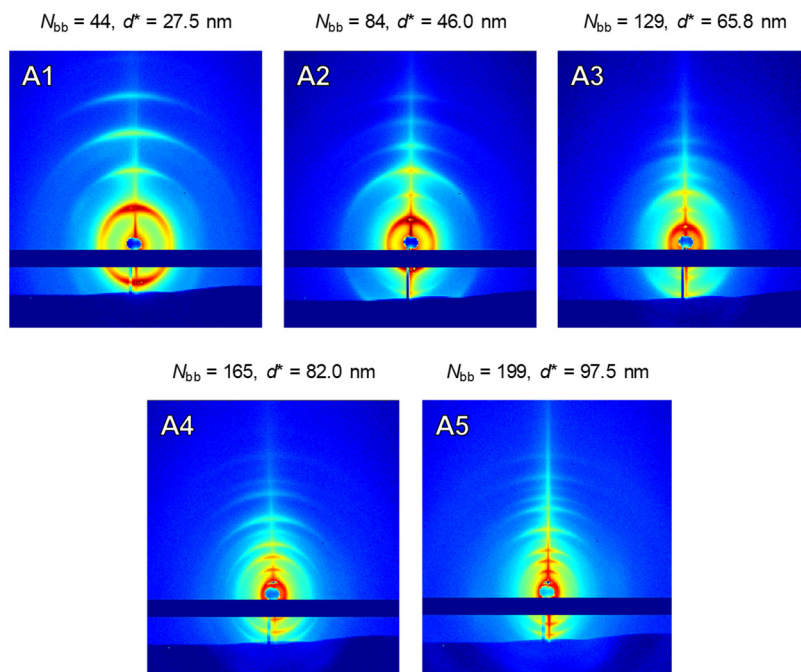
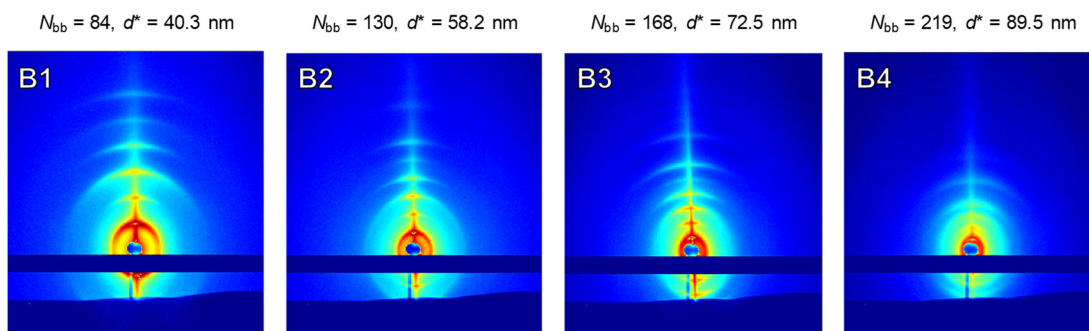
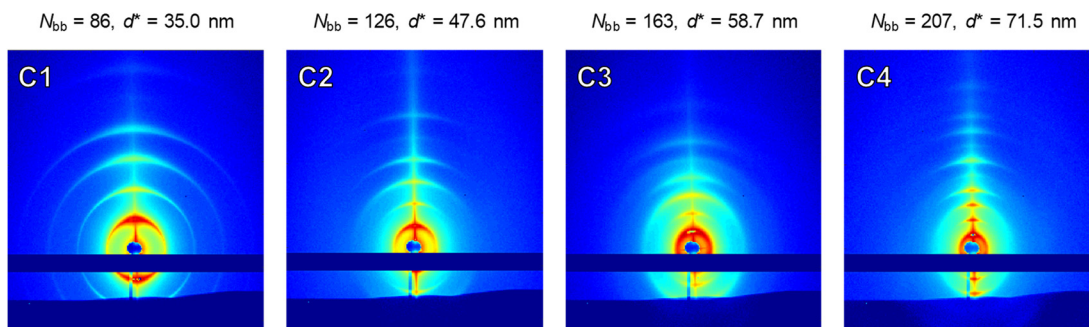
**B-2 Supporting Data: Graft Distribution and Block Polymer Self-Assembly**

**Figure B.2:** SEC traces for graft block polymers **BP-1**, **BP-2**, and **BP-3**, indicating essentially identical molecular weights and dispersities.



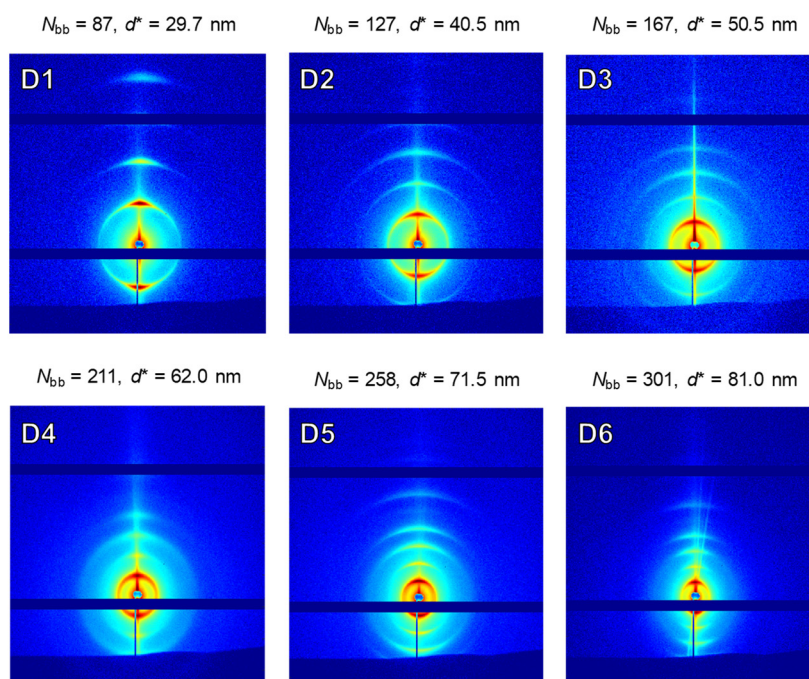
**Figure B.3:**  $^1\text{H}$  NMR data for graft block polymers **BP-1**, **BP-2**, and **BP-3**, indicating essentially identical chemical compositions ( $f \approx 0.5$ ).

### B-3 Supporting Data: Grafting Density and Block Polymer Self-Assembly

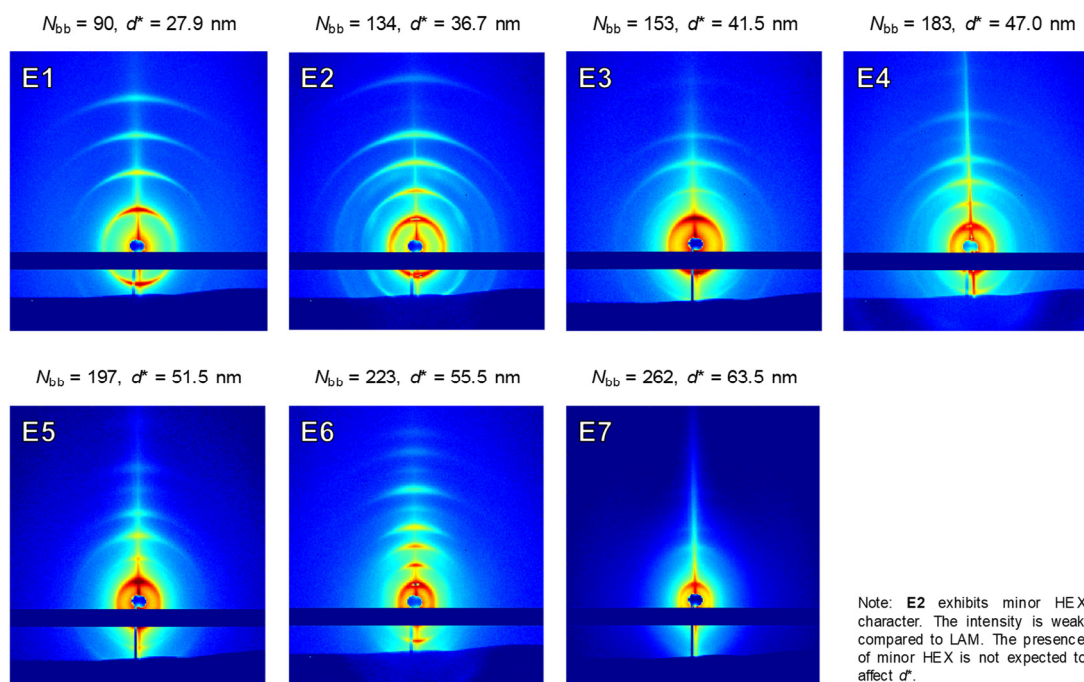
**Figure B.4 (Part 1/4):** Raw 2D SAXS data for **System I**. Compare sample IDs in Table 3.1.**System I,  $z = 1.00$** **System I,  $z = 0.75$** **System I,  $z = 0.50$** 

**Figure B.4 (Part 2/4):** Raw 2D SAXS data for **System I**. Compare sample IDs in Table 3.1.

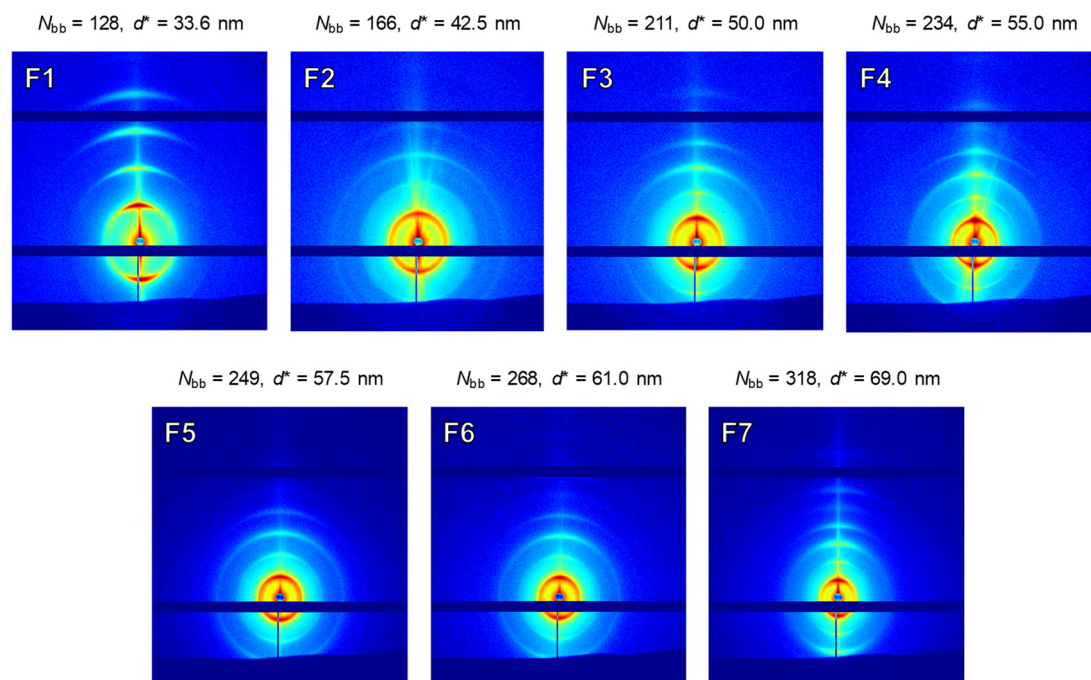
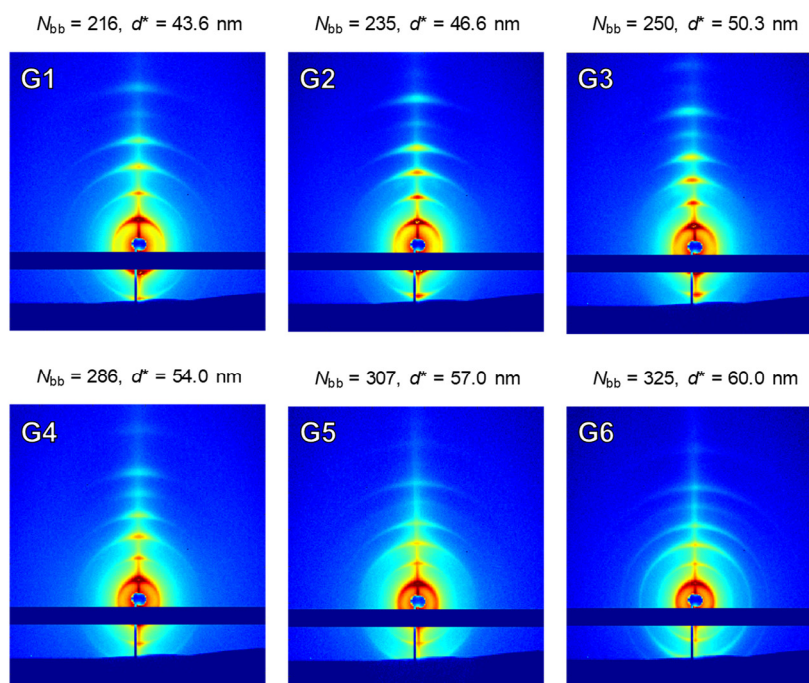
### System I, $z = 0.35$

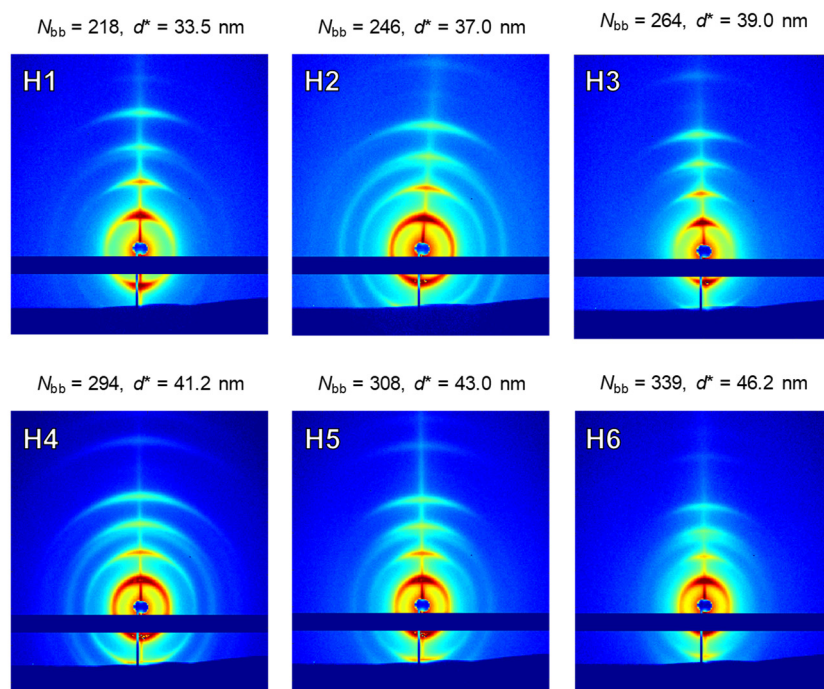


### System I, $z = 0.25$

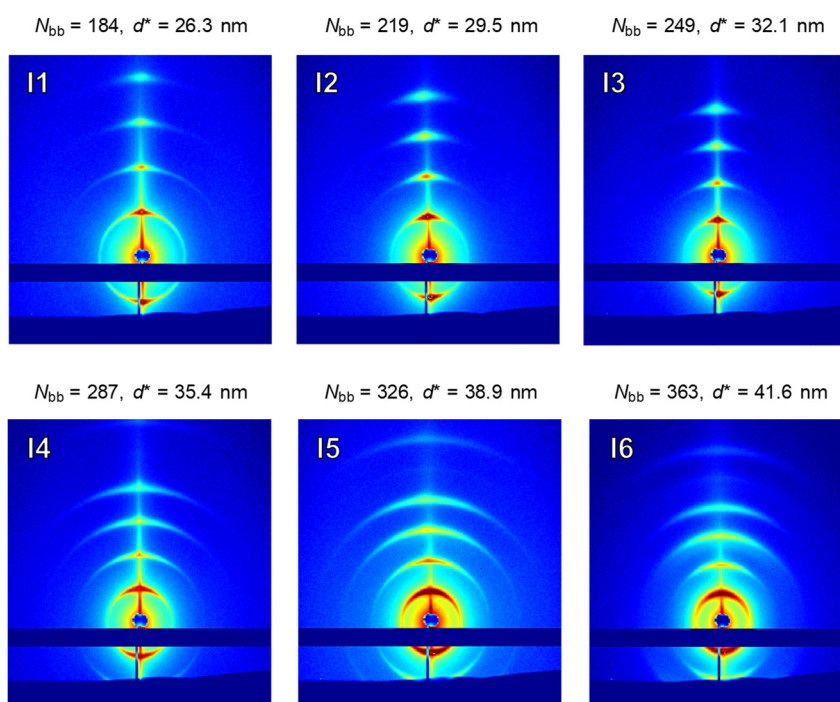




**Figure B.4 (Part 3/4):** Raw 2D SAXS data for **System I**. Compare sample IDs in Table 3.1.**System I,  $z = 0.20$** **System I,  $z = 0.15$** 

**Figure B.4 (Part 4/4):** Raw 2D SAXS data for **System I**. Compare sample IDs in Table 3.1.**System I,  $z = 0.05$** 

Note: H samples exhibit minor HEX character (*i.e.*, weak isotropic  $\sqrt{7}$  peak). The presence of minor HEX is not expected to affect  $d^*$ .

**System I,  $z = 0$** 

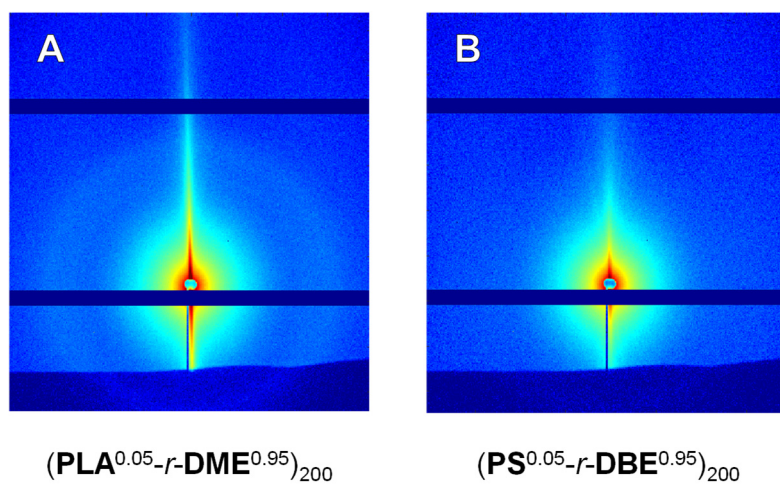
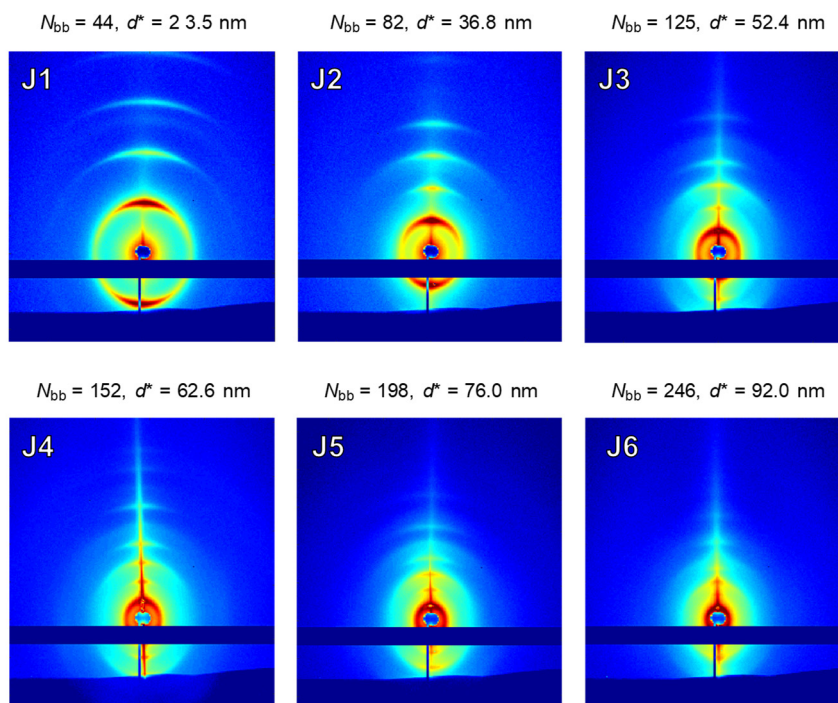


**Figure B.5:** Raw 2D SAXS data for  $z = 0.05$  graft polymers: (a)  $(\text{PLA}^{0.05}\text{-}r\text{-DME}^{0.95})_{200}$ , (b)  $(\text{PS}^{0.05}\text{-}r\text{-DBE}^{0.95})_{200}$ . These polymers correspond to each block of the lowest-grafting-density samples investigated herein. Even at large  $N_{\text{bb}}$ , no evidence of microphase separation is observed, suggesting that each block is effectively homogeneous. To a first approximation,  $\chi$  between the backbone and side chains does not appear significant.

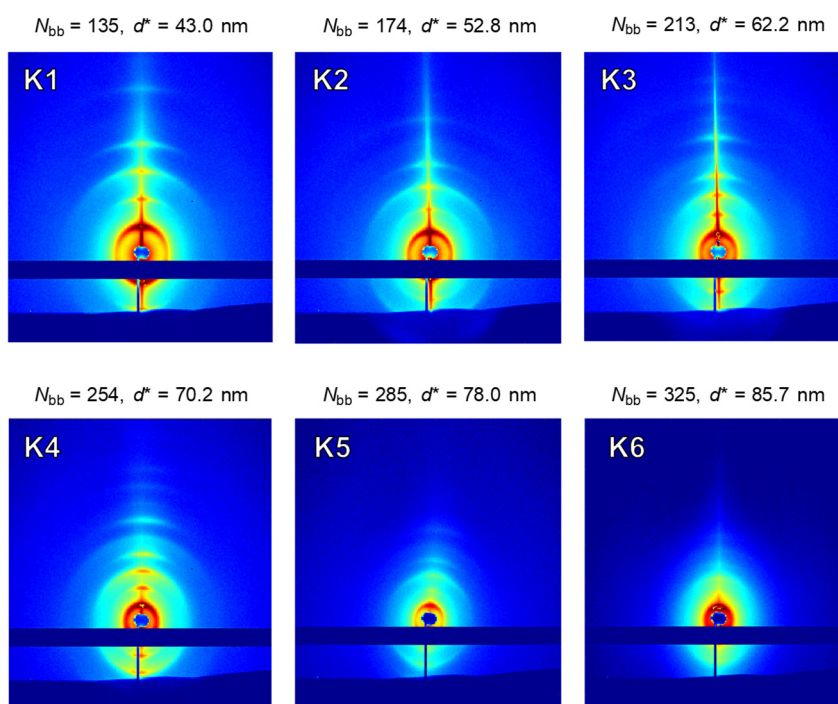


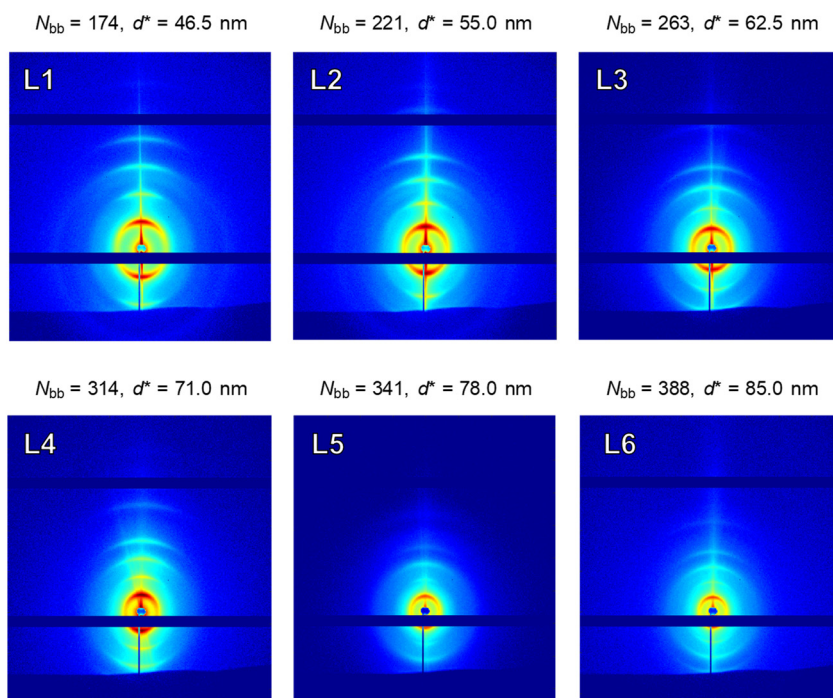
**Figure B.6 (Part 1/4):** Raw 2D SAXS for **System II**. Compare sample IDs in Table 3.2.

### System II, $z = 0.75$

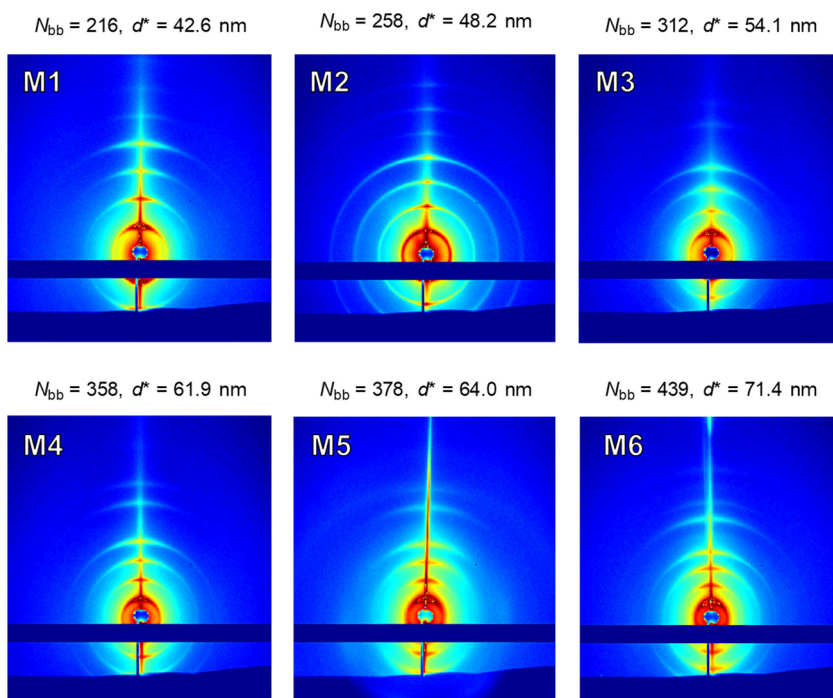


### System II, $z = 0.50$



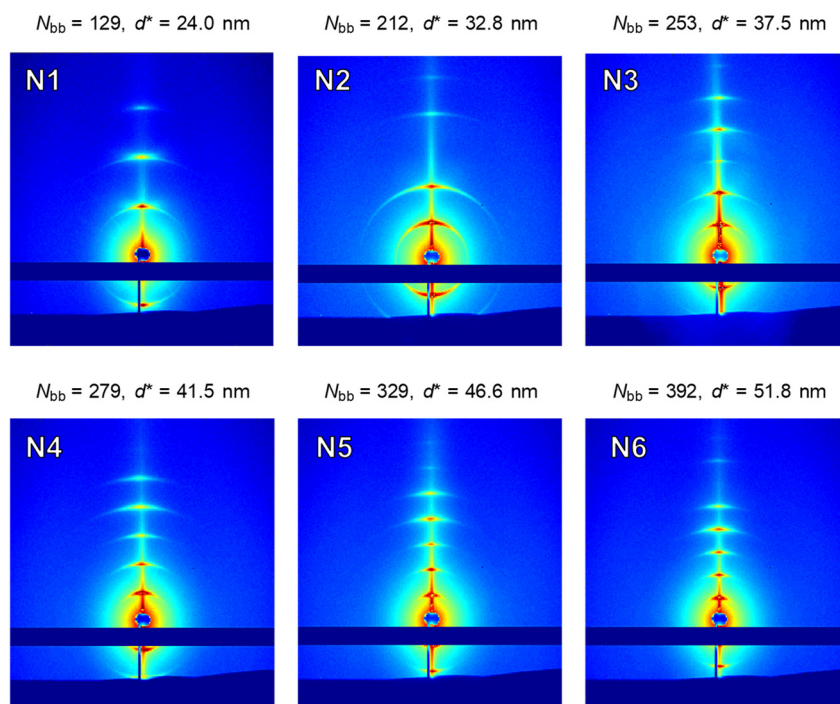
**Figure B.6 (Part 2/4):** Raw 2D SAXS for **System II**. Compare sample IDs in Table 3.2.**System II,  $z = 0.35$** 

Note: L1–L2 exhibit minor HEX character (*i.e.*, weak  $\sqrt{7}$  peak). The presence of minor HEX is not expected to affect  $d^*$ .

**System II,  $z = 0.25$** 

**Figure B.6 (Part 3/4):** Raw 2D SAXS for **System II**. Compare sample IDs in Table 3.2.

### System II, $z = 0.15$



### System II, $z = 0.12$

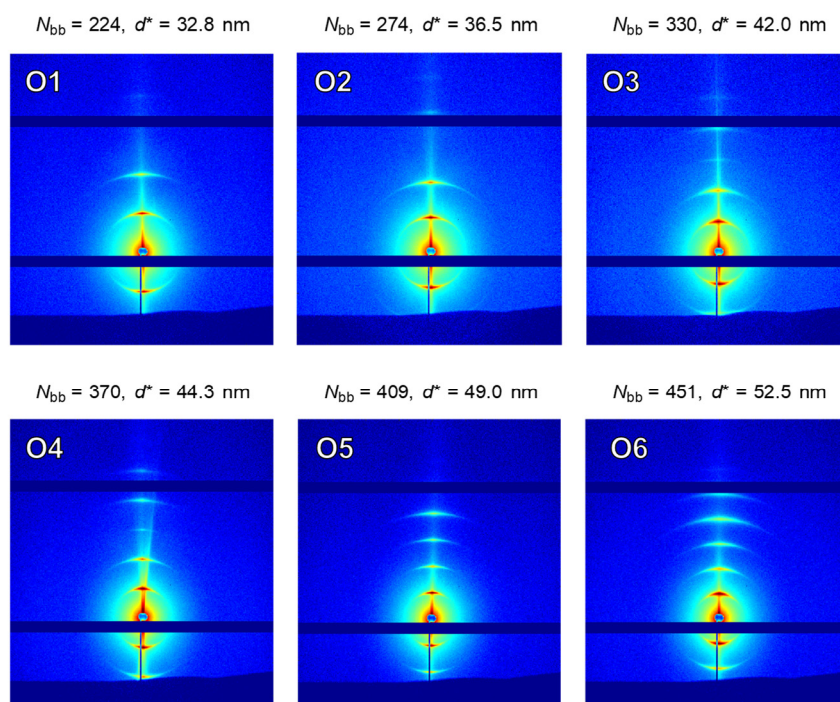
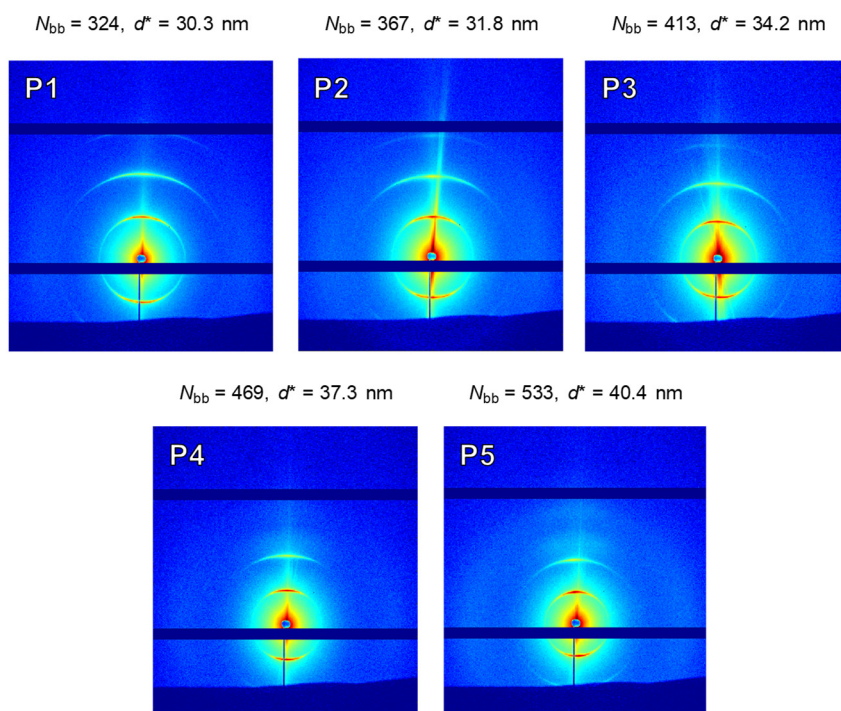


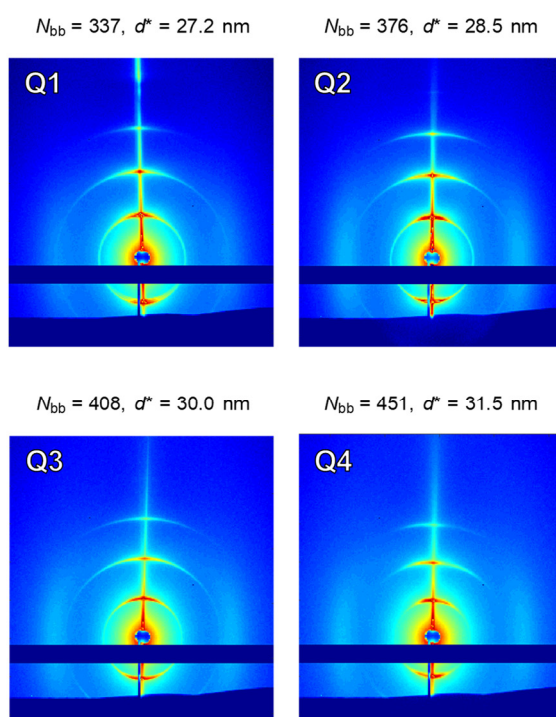


**Figure B.6 (Part 4/4):** Raw 2D SAXS for **System II**. Compare sample IDs in Table 3.2.

### System II, $z = 0.06$

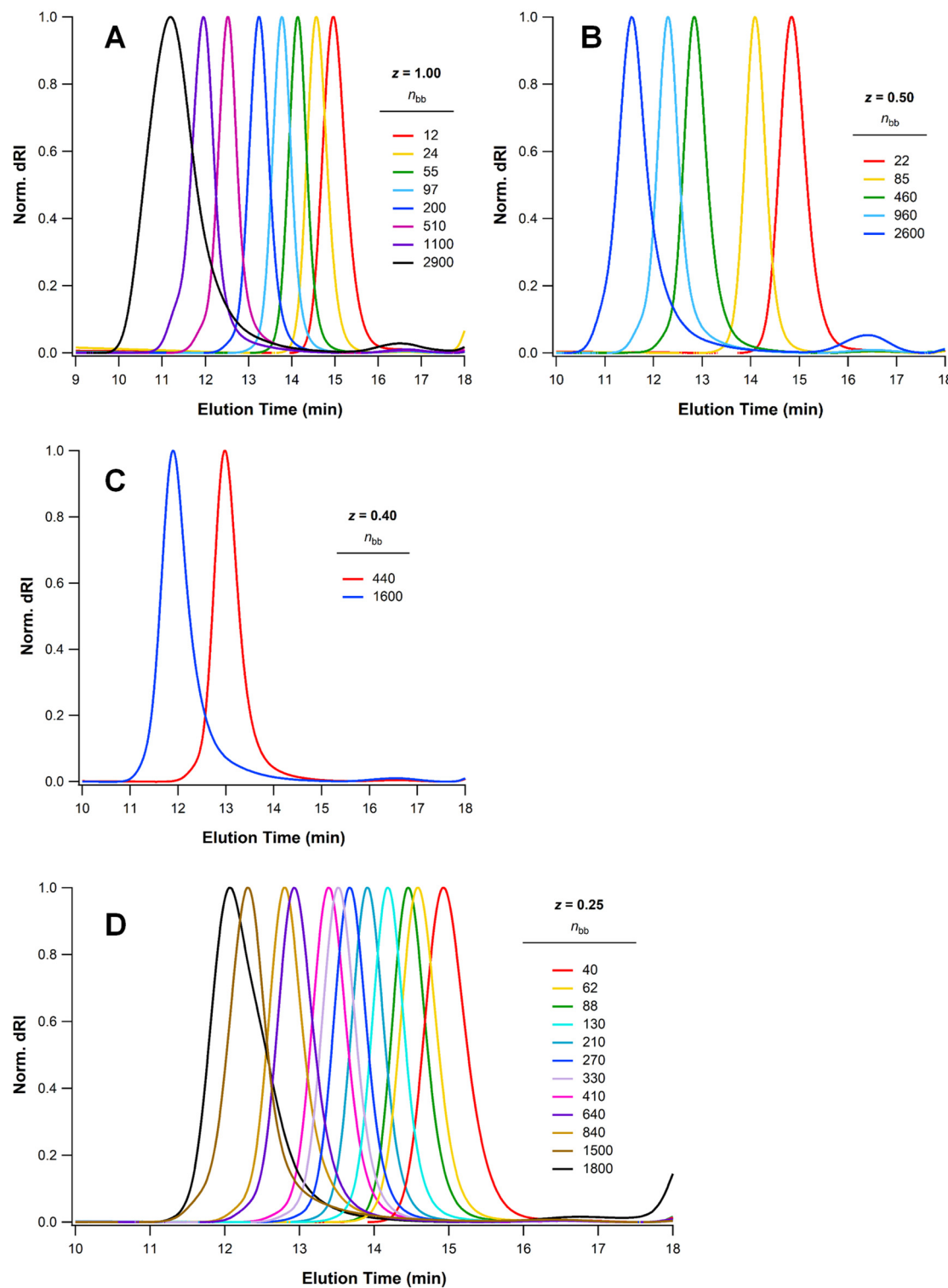


### System II, $z = 0.05$

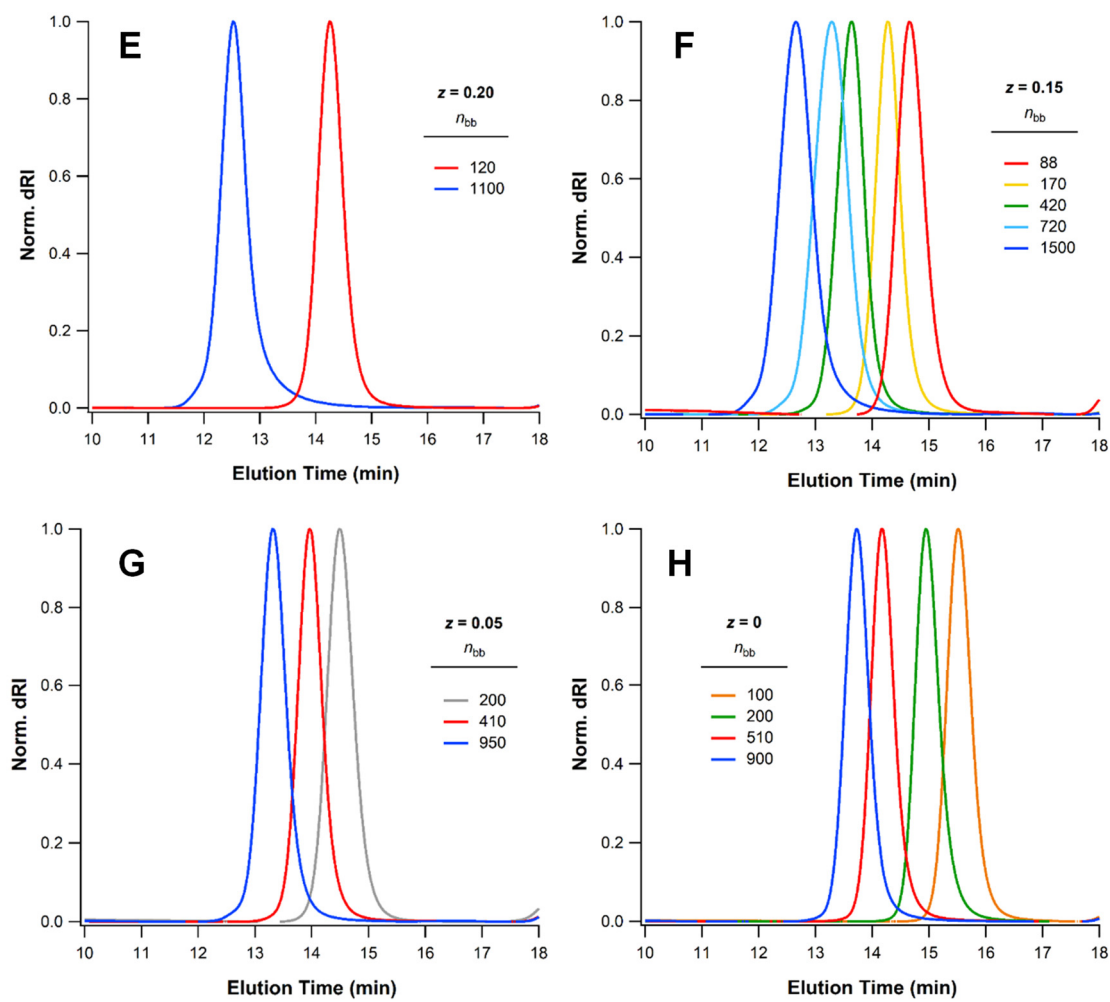


## B-4 Supporting Data: Grafting Density and Linear Rheology

**Figure B.7 (Part 1/2):** SEC traces for  $(\text{PLA}^z\text{-}r\text{-DME}^{1-z})_n$  graft polymers, where  $z = (A)$  1.00,  $(B)$  0.50,  $(C)$  0.40, or  $(D)$  0.25.



**Figure B.7 (Part 2/2):** SEC traces for  $(\text{PLA}^z\text{-}r\text{-DME}^{1-z})_n$  graft polymers, where  $z = (E) 0.20$ ,  $(B) 0.15$ ,  $(C) 0.05$ , or  $(D) 0$ .



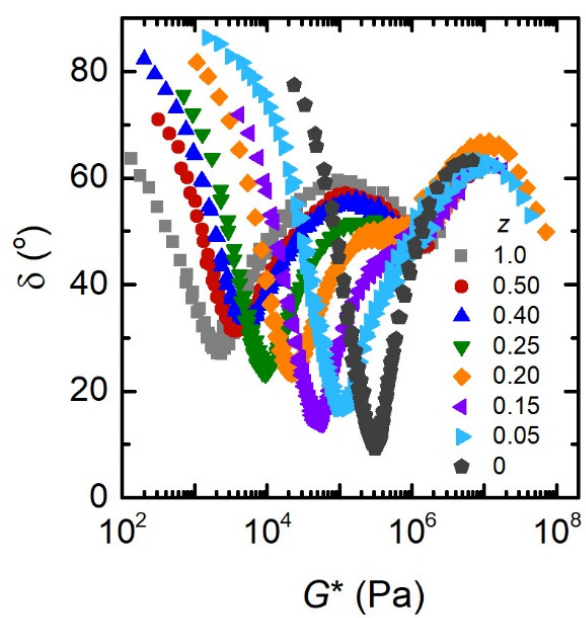


**Figure B.8:** Van Gurp-Palmen plots of the highest- $M_w$  (*i.e.*, most-entangled) sample for each  $z$ .